Carbohydrate Polymers 91 (2013) 518–528

Contents lists available at SciVerse ScienceDirect

Carbohydrate Polymers

journal homepage: www.elsevier.com/locate/carbpol

Green synthesis of gold nanoparticles using a glucan of an edible mushroom and study of catalytic activity

Ipsita K. Sen, Kousik Maity, Syed S. Islam*

Department of Chemistry and Chemical Technology, Vidyasagar University, Midnapore 721102, West Bengal, India

ARTICLE INFO

Article history:
Received 2 May 2012
Received in revised form 16 August 2012
Accepted 18 August 2012
Available online 25 August 2012

Keywords:
Gold nanoparticles
Bioconjugates
4-Nitrophenol
Reduction
Pseudo-first-order kinetics

ABSTRACT

Gold nanoparticles were synthesized by reducing chloroauric acid with a glucan, isolated from an edible mushroom *Pleurotus florida*, cultivar Assam Florida. Here, glucan acts as reducing as well as stabilizing agent. The synthesized gold nanoparticles were characterized by UV–visible spectroscopy, HR-TEM, XRD, SEM, and FT-IR analysis. The results indicated that the size distribution of gold nanoparticles (Au NPs) changed with the change in concentration of chloroauric acid ($HAuCl_4$). The resulting Au NPs-glucan bioconjugates function as an efficient heterogeneous catalyst in the reduction of 4-nitrophenol (4-NP) to 4-aminophenol (4-AP), in the presence of sodium borohydride. The reduction of 4-nitrophenol with Au NPs-glucan bioconjugates followed pseudo-first-order kinetics. The effect of particle size and gold loading on reduction rate of 4-NP was studied with Au NPs-glucan bioconjugates prepared with different concentrations of $HAuCl_4$. The synthesis of catalytically active Au NPs using a pure mushroom polysaccharide of known structure is reported for the first time.

1. Introduction

In recent years, metal nanoparticles have been studied extensively because of their unusual physical and chemical properties, leading to their enormous applications in catalysis, optics, electronics, and biotechnology (Cao, Jin, & Mirkin, 2001; Hayward, Saville, & Aksay, 2000; Pradhan, Pal, & Pal, 2001, 2002; Zeng et al., 2007). Most of the routes for the synthesis of metal nanoparticles involved the use of chemical reducing agents like sodium borohydride, N,N-dimethyl formamide, trisodium citrate, or other organic compounds (Pastoriza-Santos & Liz-Marzan, 1999; Rivas, Sanchez-Cortes, Garcia-Ramos, & Morcillo, 2001; Zeng et al., 2007). All these reducing agents possess potential environmental risk as they are associated with chemical toxicity and biological hazards. Over the past two decades, many attempts have been made keeping the aim at total elimination or minimization of waste and implementation of sustainable processes through the adoption of 12 fundamental principles of green chemistry (Anastas & Warner, 1998). Use of nontoxic chemicals, environmentally benign solvents, and renewable materials are some of the key issues that merit important consideration in a green synthetic strategy (Raveendran, Fu, & Wallen, 2003). Nowadays, biomolecules and bioorganisms are getting preference for nanoparticles synthesis because of their friendliness with environment (Esumi, Takei, & Oshimura, 2003; Mucic, Storhoff, Mirkin, & Letsinger, 1998). Raveendran et al. (2003) reported the preparation of silver nanoparticles using β-D-glucose as the reducing agent and starch as capping agent. A novel biological method for the synthesis of gold nanoparticles using the fungus *Verticillium* was reported by Mukherjee et al. (2001). Philip (2009) reported biosynthesis of Au, Ag and Au–Ag nanoparticles using edible mushroom extract.

Polysaccharides from the fruit bodies of mushroom have drawn the attention in the area of biochemistry and pharmaceutical science because of their immunostimulatory, anti-tumor, antidiabetic, and antioxidant properties (Maity et al., 2010; Roy et al., 2009; Tong et al., 2009). Besides the above mentioned properties they can also play an important role in nanoscience because these polysaccharide molecules can easily synthesize metal nanoparticles by reducing their corresponding metal salts and can also function as an excellent template for nucleation and stabilization of nanoparticles. In recent past, Vigneshwaran, Kathe, Varadarajan, Nachane, and Balasubramanya (2007) reported the synthesis of Ag-protein (core–shell) nanoparticles using spent mushroom substrate (SMS). Here, the substrate reduced silver ions to produce silver nanoparticles and the protein secreted by the fungus play the role of protecting agent. But, this report failed to explain clearly which part of the SMS is responsible for the reduction of silver ions and also unable to speak about the path of reaction. Here, we are reporting the synthesis of Au NPs using a (1 → 3)-, (1 → 6)-α, β-D-glucan (Roy

* Corresponding author. Tel.: +91 03222 276558x437; fax: +91 03222 275329; mobile: +91 9932629971.
E-mail address: sirajul_1999@yahoo.com (S.S. Islam).

0144-8617/$ – see front matter © 2012 Elsevier Ltd. All rights reserved.
http://dx.doi.org/10.1016/j.carbpol.2012.08.058

et al., 2009) isolated from an edible mushroom *Pleurotus florida*, cultivar Assam Florida, which act as reducing as well as capping agent.

Nitroaromatic compounds have been found to be toxic or mutagenic to many life forms. For example, 2,4,6-trinitrotoluene (TNT), 2,4-dinitro toluene (2,4-DNT), 1,3-dinitrobenzene and nitrophenols have shown that they can cause hepatitis and anemia (MaConnell & Flinn, 1946; Nay, Randall, & King, 1974). Nitrophenols among the most common and versatile organic pollutant, are widely used in the chemical industry and are listed as priority pollutants by the U.S. EPA. 4-Nitrophenol (4-NP) is highly stable in water and takes a long time to degrade, posing environmental risk by exhibiting carcinogenic activities. Because of the environmental hazards caused by 4-NP contaminating in industrial and agricultural waste water, much attention has been given on its degradation. Many processes have been employed for the removal of nitrophenols including adsorption (Marais & Nyokong, 2008), photocatalytic degradation (Bo, Zhang, Quan, & Zhao, 2008), microwave assisted degradation (Oturan, Peiroten, Chartrin, & Acher, 2000), and so on. But, all the above processes are energy consuming and involve the use of organic solvents. So, in the present scenario, it is very important to develop aqueous phase conversion of 4-NP to 4-AP under mild conditions.

Metal nanoparticles with size in the nanometer range have higher Fermi potential which leads to the lowering of reduction potential value and hence metal nanoparticles can function as catalyst for many electron transfer reactions (Cao et al., 2001; Ghosh, Mandal, Kundu, Nath, & Pal, 2004). Study on the catalytic activity of gold nanoparticles has become a hot topic of research after the discovery that gold nanoparticles are an excellent catalyst for CO oxidation at low temperature (Haruta, Kobayashi, Sano, & Yamada, 1987). Corma and Serna (2006) reported the selective reduction of nitro groups in the presence of other reducible functions catalyzed by gold nanoparticles supported on TiO_2 and Fe_2O_3. Narayanan and Sakthivel (2011) reported heterogeneous catalytic degradation of 4-nitrophenol using fungal-matrixed gold nanocomposites. Here, we have carried out the catalytic conversion of 4-NP to 4-AP with the help of Au NPs-glucan bioconjugates, synthesized using a glucan isolated from an edible mushroom *P. florida*, cultivar Assam Florida. Since, the recent trends in nanotechnology give emphasis on the use of biological entities in place of chemical reagents for nanoparticles synthesis, the use of a mushroom polysaccharide (glucan) in the synthesis of Au NPs and application of the resulting Au NPs-glucan bioconjugates as heterogeneous catalyst in the degradation of toxic pollutant like 4-nitrophenols will definitely draw a considerable attention in the field of nanotechnology.

2. Materials and methods

2.1. Materials

All the reagents purchased were of analytical grade and used as received. 4-Nitrophenol was purchased from Loba Chemie, chloroauric acid ($HAuCl_4$) was purchased from Sigma–Aldrich and sodium borohydride ($NaBH_4$) was provided by Merck Ltd. All aqueous solutions were prepared by using deionized double distilled water.

2.2. Synthesis of gold nanoparticles

Fresh fruit bodies of the mushroom, *P. florida*, cultivar Assam Florida were boiled in distilled water, centrifuged and the filtrate was precipitated in alcohol to get crude polysaccharide which was further purified through Sepharose-6B column as adopted in our earlier work (Roy et al., 2009). The structure of the pure polysaccharide was confirmed as (1 → 3)-, (1 → 6)-α, β-D-glucan (Roy et al., 2009) and used for Au NPs synthesis. In a typical one step synthesis protocol, 60 mL of 0.05% (w/v) glucan solution was prepared by using double distilled water. Twenty milliliters of 1 mM $HAuCl_4$ was then added to it and stirred on a magnetic stirrer in 70 °C water bath and the transformation of chloroaurate ions to Au NPs was monitored using UV–visible spectrophotometer. Au NPs-glucan bioconjugates with different gold loadings were synthesized by using another two different concentration of $HAuCl_4$ (0.5 mM, and 1.5 mM) keeping other conditions unchanged.

An aqueous solution of $HAuCl_4$ (5 mL, 1 mM) was mixed with 15 mL of varying concentrations of 0.02%, 0.04% and 0.08% (w/v) of glucan and the mixture was then heated to 70 °C under magnetic stirrer using a water bath and the formation of Au NPs was monitored using UV–visible spectrophotometer.

2.3. Characterization of gold nanoparticles

2.3.1. UV–visible spectral analysis

Change in color was observed in the chloroauric acid solution mixed with glucan as heating was continued and the UV–visible spectra of this solution were recorded in a 1-cm path length quartz cuvette with a Shimadzu UV–visible 1601 spectrophotometer.

2.3.2. High resolution-transmission electron microscopy (HR-TEM) analysis

High resolution-transmission electron microscopic images were recorded in a JEOL-JEM-2100 HRTEM operated at 200 kV. For the TEM analysis a droplet of aqueous solution of synthesized Au NPs was spread onto a carbon coated copper grid (300 meshes) and dried under IR lamp. Micrographs were taken both in the transmission mode and in the diffraction mode.

2.3.3. X-ray diffraction (XRD) analysis

A thin film of the sample was prepared on a microscopic glass slide using the aqueous solution of the glucan embedded with Au NPs and measurements were carried out with a Rigaku Miniflex II X-ray diffractometer, using Ni-filtered Cu Kα ($\lambda = 0.15406$ nm) radiation. The diffraction intensities were recorded from 30° to 80° 2θ angle.

2.3.4. Field emission-scanning electron microscopy (FE-SEM) and Fourier transform-infrared (FT-IR) spectra analysis

Morphology of the synthesized Au NPs was analyzed by FE-SEM techniques. For the FE-SEM analysis, solution of Au NPs in water was drop-cast on microscopic glass slides and coated with platinum to reduce charging, dried in air at 25 °C and finally under vacuum. The micrographs were taken in an FE-SEM instrument (JEOL, JSM 6700 F) operating at 5 kV. The aqueous solution of the synthesized Au NPs was freeze-dried and the dried sample was used for FT-IR analysis. FT-IR analysis of the dried sample was performed in an FT-IR-8400S (Shimadzu) instrument between 4000 and 400 cm^{-1} using KBr pellet technique.

2.4. Thermogravimetric analysis (TGA)

Thermogravimetric analysis (TGA) of glucan and Au NPs-glucan bioconjugates was carried out in the temperature range of 27 °C (room temperature) to 510 °C on a Shimadzu DTG-60 thermal analyzer in nitrogen atmosphere. The heating rate was 10 °C min^{-1}.

2.5. Heterogeneous catalysis of Au NPs-glucan bioconjugates in 4-nitrophenol reduction

The reduction of 4-nitrophenol by $NaBH_4$ was performed as a model reaction to investigate the catalytic activity of Au

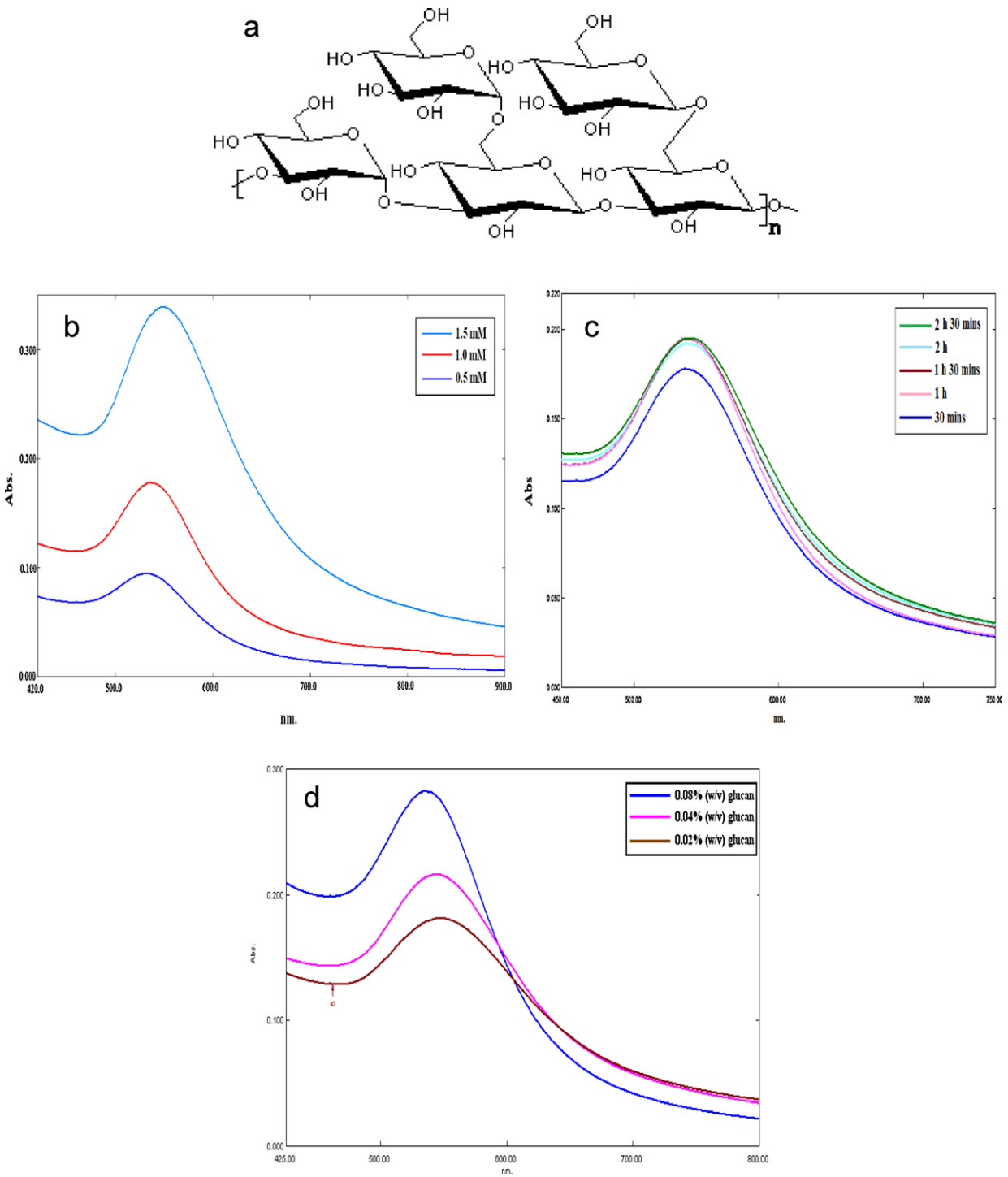

Fig. 1. Structure of (1 → 3)-, (1 → 6)-α, β-D-glucan, a polysaccharide obtained from the aqueous extract of an edible mushroom *Pleurotus florida*, cultivar Assam Florida (a). UV–visible spectra of Au NPs prepared with 0.5 mM, 1.0 mM and 1.5 mM $HAuCl_4$ and 0.05% (w/v) glucan in a 70 °C water bath taken after 1 h 30 min. The peaks around 530 nm correspond to surface plasmon resonance of Au NPs (b). UV–visible spectra of Au NPs prepared with 1.0 mM $HAuCl_4$ and 0.05% (w/v) glucan taken at different time interval (c). UV–visible spectra of Au NPs prepared with 1.0 mM $HAuCl_4$ and different concentrations e.g. 0.08%, 0.04%, and 0.02% (w/v) glucan (d).

NPs-glucan bioconjugates. The effect of particle size and gold loading on rate of reduction of 4-NP was studied by using Au NPs-glucan bioconjugates as catalyst prepared with three different concentrations of chloroauric acid (0.5 mM, 1.0 mM, and 1.5 mM). The catalytic reaction was carried out in 1-cm path length cuvette. Two milliliters of double distilled water and 1 mL of 15 mM $NaBH_4$ were first taken in the cuvette, thereafter 120 μL of 2 mM 4-NP was added to it followed by the addition of 3.5 mg of freeze dried Au NPs-glucan bioconjugates. Immediately after the addition of Au NPs-glucan bioconjugates, the color change was measured by taking UV–visible spectra in 2-min interval in the range of 200–600 nm at room temperature (25 °C). The Au NPs catalyst prepared with 1.0 mM $HAuCl_4$ was recovered at the end of the reaction by centrifugation and redispersed in deionized double distilled water for three times to reuse them in successive cycles.

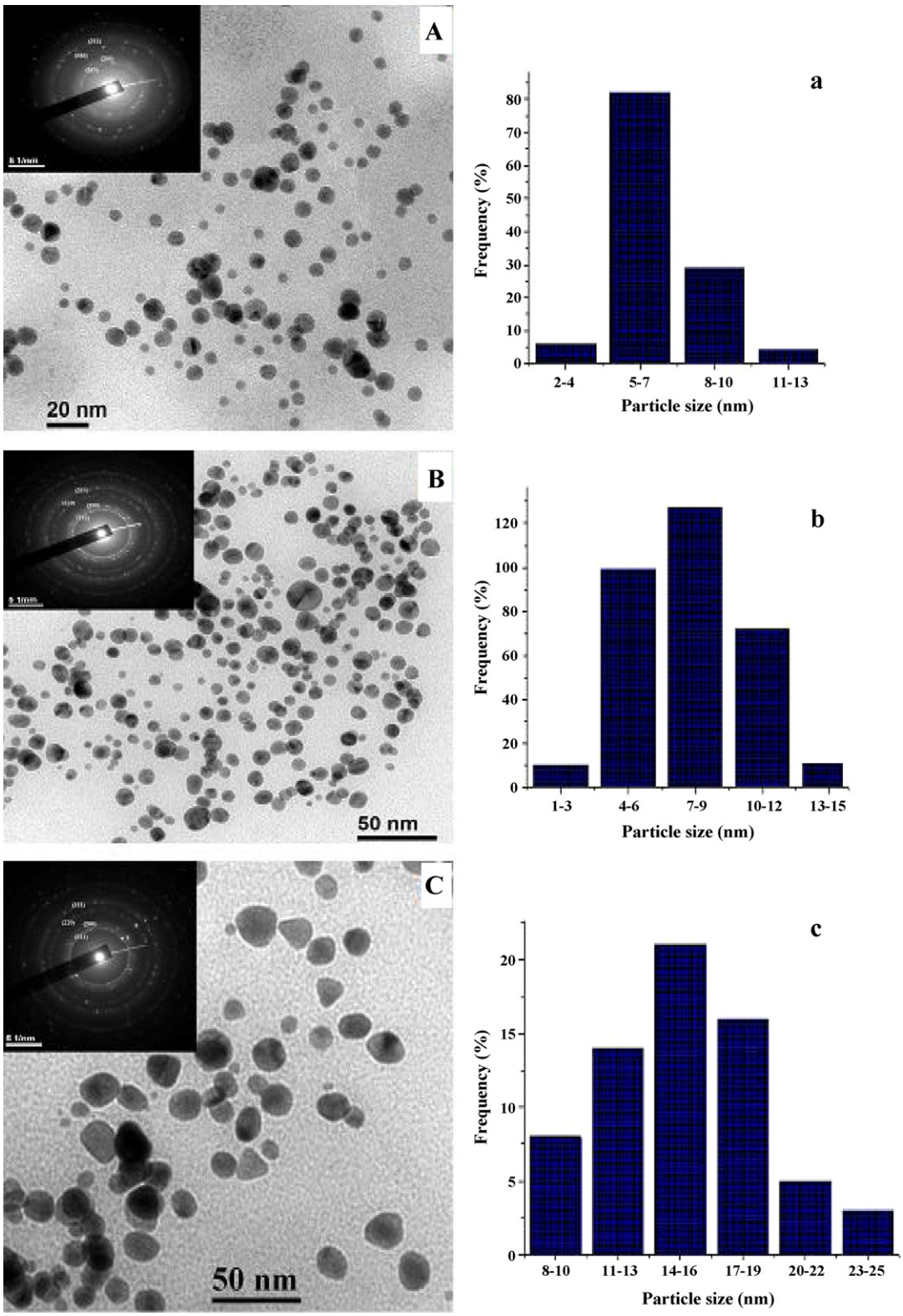

Fig. 2. TEM images and the corresponding selected area electron diffraction (SAED) patterns (inset) of Au NPs prepared with 0.05% (w/v) glucan and 0.5 mM $HAuCl_4$ (A), 1.0 mM $HAuCl_4$ (B), and 1.5 mM $HAuCl_4$ (C). Particle size distribution histograms of Au NPs prepared with 0.05% (w/v) glucan and 0.5 mM $HAuCl_4$ (a), 1.0 mM $HAuCl_4$ (b), and 1.5 mM $HAuCl_4$ (c). HR-TEM images of Au NPs prepared with 0.5 mM $HAuCl_4$ (d), 1.0 mM $HAuCl_4$ (e), and 1.5 mM $HAuCl_4$ (f) showing clear lattice fringes reveal that the growth of Au NPs occurred preferentially on the (1 1 1) plane.

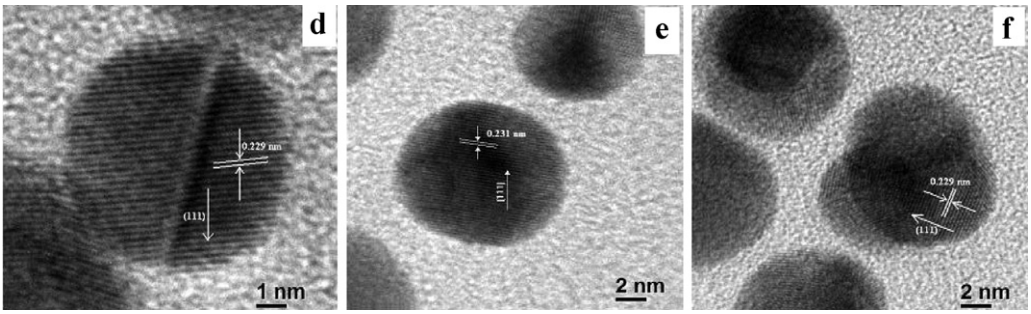

Fig. 2. (*Continued*)

3. Results and discussion

3.1. Characterization of gold nanoparticles

3.1.1. UV–visible spectral analysis

A $(1 \rightarrow 3)$-, $(1 \rightarrow 6)$-α, β-D-glucan (Fig. 1a) isolated from *P. florida*, cultivar Assam Florida was used for Au NPs synthesis. Au NPs were synthesized by reducing 0.5 mM, 1.0 mM, and 1.5 mM $HAuCl_4$ with 0.05% (w/v) glucan solution. The UV–visible spectra of the solutions taken after 1.5 h heating in 70 °C water bath are shown in Fig. 1b. All the spectra exhibit an absorption band around 530 nm, which is a typical plasmon resonance band of Au NPs (Tsutsui, Hayakawa, Kawamura, & Nogami, 2011). The absorption peak width gradually becomes narrower with the decrease in concentration of $HAuCl_4$ from 1.5 mM to 0.5 mM suggesting the size distribution of Au NPs becomes narrower (Babapour, Akhavan, Azimirad, & Moshfeg, 2006) with the decrease in concentration of $HAuCl_4$. Moreover, it has been noticed that the absorption intensity gradually increases with the increase in concentration of $HAuCl_4$ from 0.5 mM to 1.5 mM suggesting the formation of greater number of nanoparticles with higher concentration of $HAuCl_4$. The variation of intensity of the plasmon resonance may also be attributed to the cluster size (Schmid, 2001). Fig. 1c shows the UV–visible spectra of Au NPs synthesized by using 1.0 mM $HAuCl_4$ and 0.05% (w/v) glucan taken at different time intervals. Intensity of plasmon resonance gradually increased as the reaction was continued up to 1 h 30 min and thereafter no change in intensity was observed indicating almost complete reduction of Au^{3+} to Au^0. The UV–visible spectra of Au NPs prepared with different concentrations of glucan are presented in Fig. 1d which shows that the SPR band of the synthesized Au NPs blue-shifted from 546 to 535 nm with increasing glucan concentration from 0.02% to 0.08% (w/v) indicating that the particle size was decreased with increasing glucan concentration.

3.1.2. High resolution-transmission electron microscopy (HR-TEM) analysis

To look into the size and morphology of the synthesized nanoparticles, transmission electron microscopy (TEM) analysis was done. Typical TEM images and their corresponding particle size distribution histograms are shown in Fig. 2A–C and Fig. 2a–c respectively. The average particle size was analyzed as 5.33 ± 1.18, 8.01 ± 2.67, and 14.93 ± 2.88 nm when 0.5, 1.0, and 1.5 mM $HAuCl_4$ respectively were reduced with glucan (0.05%). The typical HR-TEM images (Fig. 2d–f) with clear lattice fringes revealed that the growth of Au NPs occurred preferentially on the (1 1 1) plane. The SAED patterns (inset Fig. 2A–C) of the Au NPs indexed to the (1 1 1), (2 0 0), (2 2 0), and (3 1 1) Bragg reflections of face-centered cubic (fcc) structure. HR-TEM images and the SAED patterns with circular rings corresponding to the above planes indicate high crystalline nature of the synthesized Au NPs.

An increase in particle size and particle size distribution was noted with the increase in the concentration of $HAuCl_4$ from 0.5 mM to 1.5 mM. This can be explained by considering the role of glucan as stabilizer or nucleating agent. Here, 0.05% (w/v) glucan was used for nanoparticles synthesis. This particular concentration of glucan was sufficient to reduce 1.5 mM $HAuCl_4$ but could not protect the new born Au NPs from aggregation because this higher concentration (1.5 mM) of $HAuCl_4$ yielded greater number of Au NPs. So, with 1.5 mM $HAuCl_4$ these new born Au nanoclusters aggregated to give nanoparticles of larger size. But, with relatively low concentration (0.5 mM) of $HAuCl_4$, the same concentration of glucan (0.05%) was enough to stabilize the Au NPs and prevented further aggregation resulting in the formation of relatively smaller sized nanoparticles.

The TEM images and their corresponding particle size distribution histograms of the Au-NPs glucan conjugates prepared with different glucan concentrations varying from 0.02% to 0.08% (w/v) and fixed $HAuCl_4$ concentration (1.0 mM) are illustrated in Fig. 3A–C and Fig. 3a–c, respectively. The average particle size was found to decrease with increasing glucan concentration and analyzed to be 20.37 ± 2.82, 9.67 ± 1.93 and 6.90 ± 2.51 nm for 0.02%, 0.04% and 0.08% (w/v) glucan, respectively. This result can be verified by considering the fact that at higher concentrations glucan can effectively capped the particle surface to prevent the particle growth, resulting in smaller Au NPs whereas the glucan at very low concentration 0.02% (w/v) cannot impart proper stability to the Au NPs and the particles aggregate strongly to give clusters of larger size which are in good agreement with the findings of UV–visible spectral studies.

3.1.3. X-ray diffraction (XRD) analysis

The crystalline nature of Au NPs was further confirmed by X-ray diffraction (XRD) analysis. Fig. 4a–c shows the XRD patterns of Au NPs-glucan bioconjugates prepared with 0.5 mM, 1.0 mM, and 1.5 mM $HAuCl_4$, respectively. Four diffraction peaks at 2θ values of nearly 38.3°, 44.4°, 64.8°, and 77.8° was observed in each of the figures which correspond to (1 1 1), (2 0 0), (2 2 0), and (3 1 1) planes respectively of face-centered cubic (fcc) gold. For the Au NPs prepared with the above three concentrations of $HAuCl_4$ keeping concentration of glucan (0.05%) fixed, the observed intensity ratio of (2 0 0) to (1 1 1) diffraction peaks exhibited a relatively lower value of 0.23, 0.33, and 0.24 respectively, than the conventional bulk intensity ratio (0.52), indicating that the (1 1 1) facets were more exposed to the crystal surface of Au NPs (Philip, 2010). The lattice constant calculated from (1 1 1) diffraction pattern was 4.066 Å for the Au NPs prepared with all the three mentioned concentrations of $HAuCl_4$. The value was in close agreement with the literature report ($a = 4.0786$ Å; Joint Committee on Powder Diffraction Standards file No. 04-0784). With decrease in concentration of $HAuCl_4$ from 1.5 mM to 0.5 mM, XRD patterns of the Au NPs exhibited a gradual decrease in the peak heights with concomitant increase in the width of the peaks further supporting the gradual decrease of particle size (Narayanan & Sakthivel, 2011).

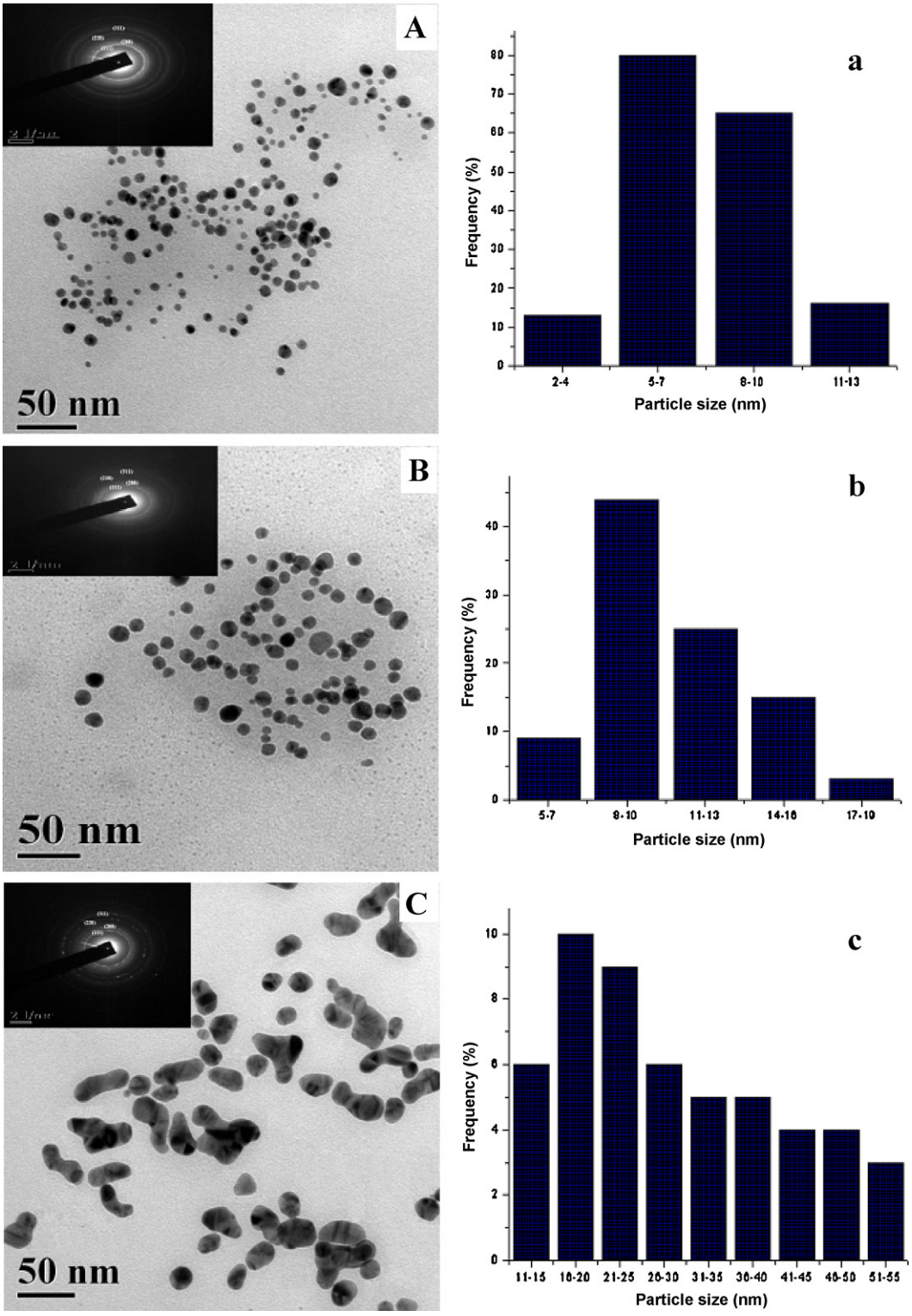

Fig. 3. TEM images and the corresponding selected area electron diffraction (SAED) patterns (inset) of Au NPs prepared with 1.0 mM $HAuCl_4$ and 0.08% (w/v) glucan (A), 0.04% (w/v) glucan (B), and 0.02% (w/v) glucan (C). Particle size distribution histograms of Au NPs prepared with 1.0 mM $HAuCl_4$ and 0.08% (w/v) glucan (a), 0.04% (w/v) glucan (b), and 0.02% (w/v) glucans (c).

3.1.4. Field emission scanning electron microscopy (FE-SEM) and Fourier transform-infrared (FT-IR) spectra analysis

Fig. 5a shows FE-SEM images of Au NPs prepared with 1.0 mM $HAuCl_4$ and 0.05% (w/v) glucan. Au NPs tend to form spherical morphology and rough surface with cluster size of about 70–500 nm. FT-IR analysis was done to enquire of the role of glucan in nanoparticles synthesis and stabilization. In the FT-IR spectrum of glucan (Fig. 5b), a broad stretching peak displayed around 3412 cm^{-1} is the characteristic for hydroxyl group and a weak band at 2924 cm^{-1} is an indication of aliphatic C—H stretching. The peaks at 1412 and 1075 cm^{-1} are possibly the bending vibrations of C—OH and the antisymmetric stretching band of

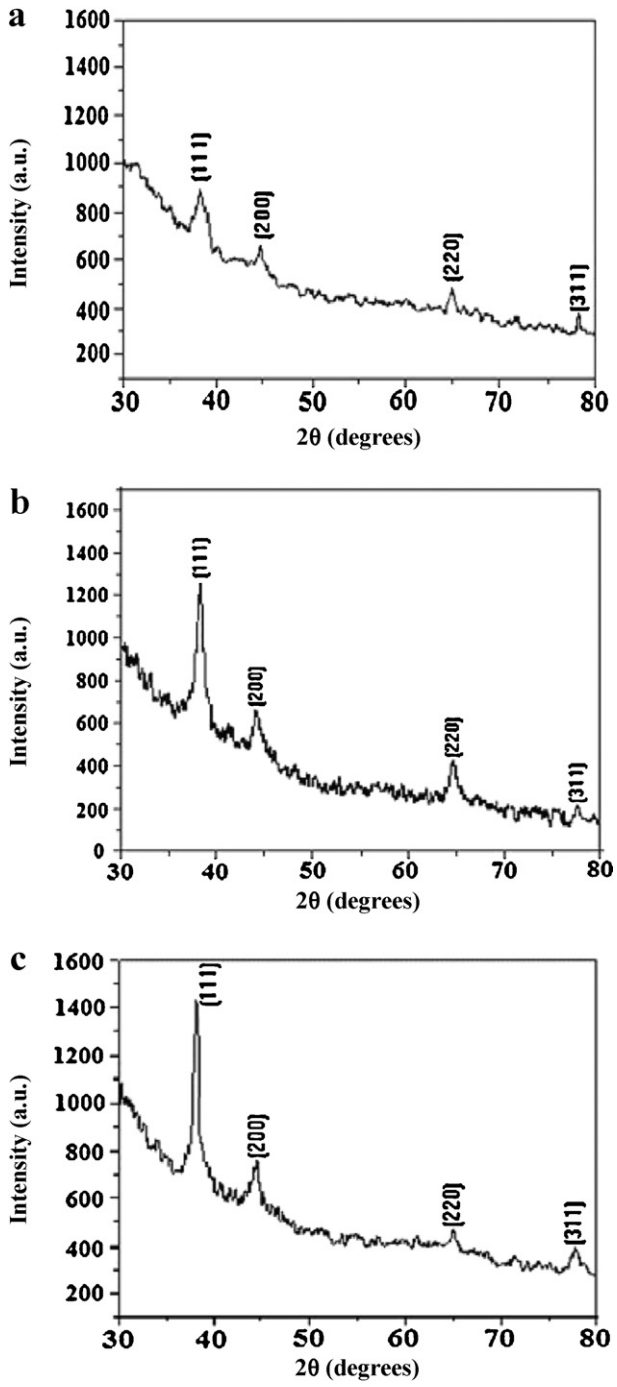

Fig. 4. XRD patterns of dried Au NPs-glucan bioconjugates prepared with 0.05 mM $HAuCl_4$ (a), 1.0 mM $HAuCl_4$ (b), and 1.5 mM $HAuCl_4$ (c). All peaks could be indexed to fcc gold.

C—O—C groups of polysaccharides (Li et al., 2007). In the FT-IR spectrum of Au NPs-glucan bioconjugates (Fig. 5c), appearance of a notch was noted in the region of 1720–1740 cm^{-1}. To get a clear view, the region between 1650 and 1740 cm^{-1} was subjected to Fourier deconvulation program which showed the presence of two small peaks at 1718 and 1738 cm^{-1} (inset in Fig. 6). Since a neutral polysaccharide (glucan) was used in this case for the synthesis of Au NPs, peaks in the region of 1720–1740 cm^{-1} would not be usually expected but the appearance of two peaks (1718 and 1738 cm^{-1}) suggests that there must be some change in the functionalities of glucan during the course of the reaction. The peaks at 1718 and 1738 cm^{-1} may be for the stretching vibrations of —COOH group and to those associated (Shi & Sun, 1988). In acidic solution of $HAuCl_4$, there would be a possibility for cleavage of some glycosidic (C—O—C) linkages of the chain of glucan and this may lead to the formation of some shorter segments with open chain structure (Sun et al., 2008). In this open chain form there would be existence of potential —CHO groups. Since, Au^{3+} ions were present in the reaction medium, these —CHO groups would be readily oxidized to —COOH groups with concomitant reduction of Au^{3+} to Au^0.

3.2. Thermogravimetric analysis (TGA)

Fig. 6 shows the thermograms of glucan and the Au NPs-glucan bioconjugates. It can be seen from the thermograms that the thermal stability of Au NPs-glucan bioconjugates was different from that of glucan. Incorporation of Au NPs in the matrix of glucan shifted the onset of the thermal decomposition toward lower temperature. At the same time, the thermograms indicate that the residual weight of Au NPs-glucan bioconjugates was almost 26% higher than that of glucan at 510 °C. A similar behavior was observed by Ag-sago starch nanocomposites (Bozanic, Djokovic, Blanusa, Nair, & Georges, 2007).

3.3. Catalytic activity of Au NPs-glucan bioconjugates in the reduction of 4-nitrophenol

To investigate the catalytic activity of Au NPs-glucan bioconjugates, at first the reduction of 4-NP with $NaBH_4$ was carried in the absence of Au NPs. It was observed that the yellow color of the solution became intense after the addition of aqueous solution of $NaBH_4$ and a red shift of the peak from 317 to 400 nm occurred. This was due to the conversion of 4-nitrophenol to 4-nitrophenolate ion in alkaline condition by the action of $NaBH_4$ (Pradhan et al., 2001). The intensity of the absorption peak at 400 nm remained unchanged even after several hours in the absence of Au NPs-glucan bioconjugates (figure not shown). Normally —NO_2 containing aromatic compounds are inert to the reduction of $NaBH_4$ (Dotzauer, Dai, Sun, & Bruening, 2006; Pradhan et al., 2001). But, immediate after the addition of freeze dried solid Au NPs-glucan bioconjugates, the reduction of 4-NP to 4-AP started which was evident from the change of yellow color of 4-nitrophenlote ion to a colorless solution of 4-AP. Appearance of a peak at 290 nm with concomitant disappearance of the peak at 400 nm confirmed the formation of 4-AP. The formation of 4-AP was finally confirmed by ^1H NMR analysis. Reaction of 4-NP with glucan and $NaBH_4$ mixture showed no change in the color and position of the absorption peak at 400 nm (figure not shown). Thus, from the above observation it can be concluded that the Au NPs-glucan bioconjugates function as a catalyst in the reduction of 4-NP.

Au NPs-glucan bioconjugates composed of branched (1 → 3)-, (1 → 6)-α, β-D-glucan (Roy et al., 2009). The free hydroxyl groups of branched chains of the glucans may help to draw the negatively charged borohydride ions (BH_4^-) and 4-nitrophenote ions closer to the surface of Au NPs. As soon as the electron donor (BH_4^-) and electron acceptor (4-nitrophenolate ion) are adsorbed on the surface of the Au NPs, catalytic reaction starts by the transfer of electron from BH_4^- to 4-nitrophenolate ion. Thus, Au NPs help in facilitating the reduction of 4-NP by lowering the activation energy of the reaction and play the role of catalyst. Since an excess of $NaBH_4$ is used in the reduction of 4-NP, it is assumed that the concentration of BH_4^- remains constant during the course of the reaction and the reaction can be considered as pseudo-first-order reaction. A good linear correlation of ln(A) versus time (Fig. 7a) was obtained and a kinetic rate constant was estimated to be 1.3×10^{-3} s^{-1} with Au NPs-glucan bioconjugates prepared at 1.0 mM $HAuCl_4$. As shown in Fig. 7b and c, similar correlation was observed for Au NPs prepared with 0.5 mM and 1.5 mM $HAuCl_4$, respectively and the rate constants

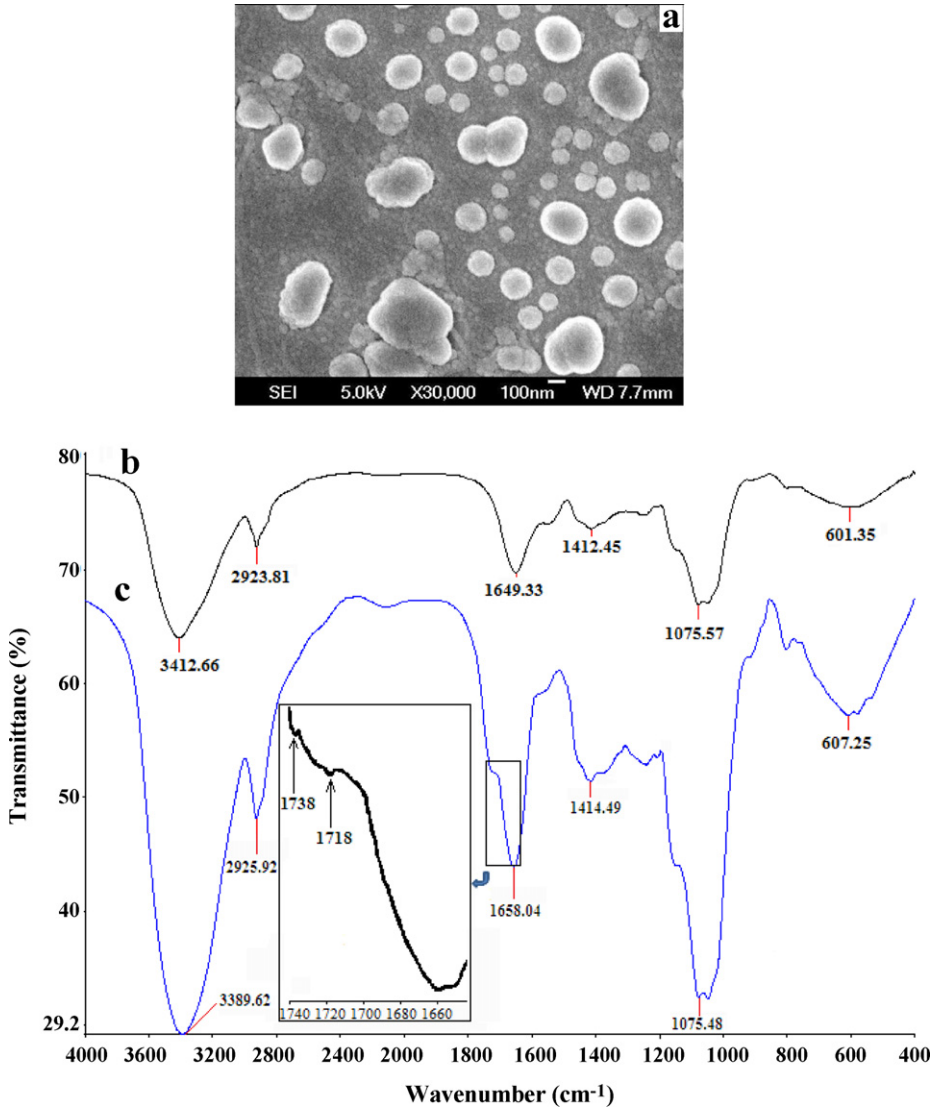

Fig. 5. FE-SEM micrograph of Au NPs prepared with 1.0 mM $HAuCl_4$ and 0.05% (w/v) glucans (a). FT-IR spectra of glucan (b) and Au NPs-glucan bioconjugates prepared with 0.05% (w/v) glucan and 1.0 mM $HAuCl_4$ (c).

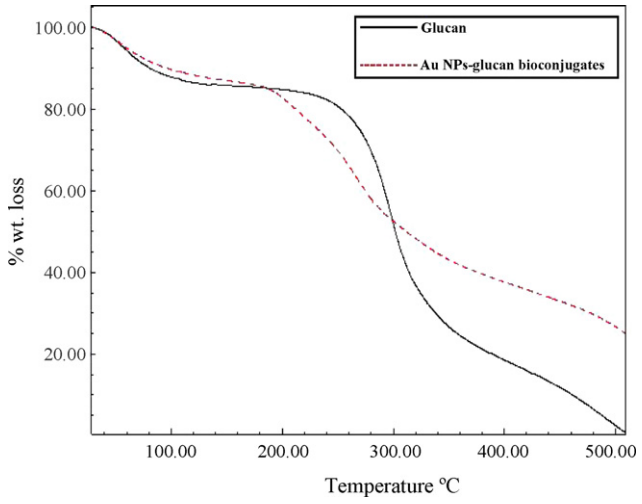

Fig. 6. TGA curves of glucan (solid line) and Au NPs-glucan bioconjugates (dashed).

were determined to be 1.9×10^{-3} and $3.3 \times 10^{-4}\ s^{-1}$, respectively (Table 1a). Rate constants for Au NPs prepared with 1.0 mM $HAuCl_4$ were calculated to be 5.6×10^{-2}/Au content/s^{-1} μmol Au^{-1} and found to be comparable with α-CD capped Au NPs (7.8×10^{-2}/Au content/s^{-1} μmol Au^{-1}) (Table 1b) as reported earlier by Huang, Meng, and Qi (2009). Although exact gold loading in the Au NPs-glucan bioconjugates could not be estimated, an increase in the color intensity of the nanoparticles solutions (Fig. 7d) indicated that gold loading increases with the increase in the concentration of $HAuCl_4$ from 0.5 mM to 1.5 mM (Wei, Ye, Jia, Yuan, & Qian, 2010). The rate of reduction of 4-NP with Au NPs-glucan bioconjugates prepared with 1.5 mM $HAuCl_4$ was expected to be greater than that prepared with 1.0 mM $HAuCl_4$ because the metal loading was higher in the former but the result was just reverse of our expectation. An increase in size of Au NPs from 8 to 15 nm with the increase in the concentration of $HAuCl_4$ from 1.0 mM to 1.5 mM was mainly responsible for the above observation. A decrease in rate with the increase in size of Au NPs was also observed when the concentration of $HAuCl_4$ was changed from 0.5 mM to 1.0 mM. Thus, the smaller sized Au NPs function as more effective catalyst than the larger

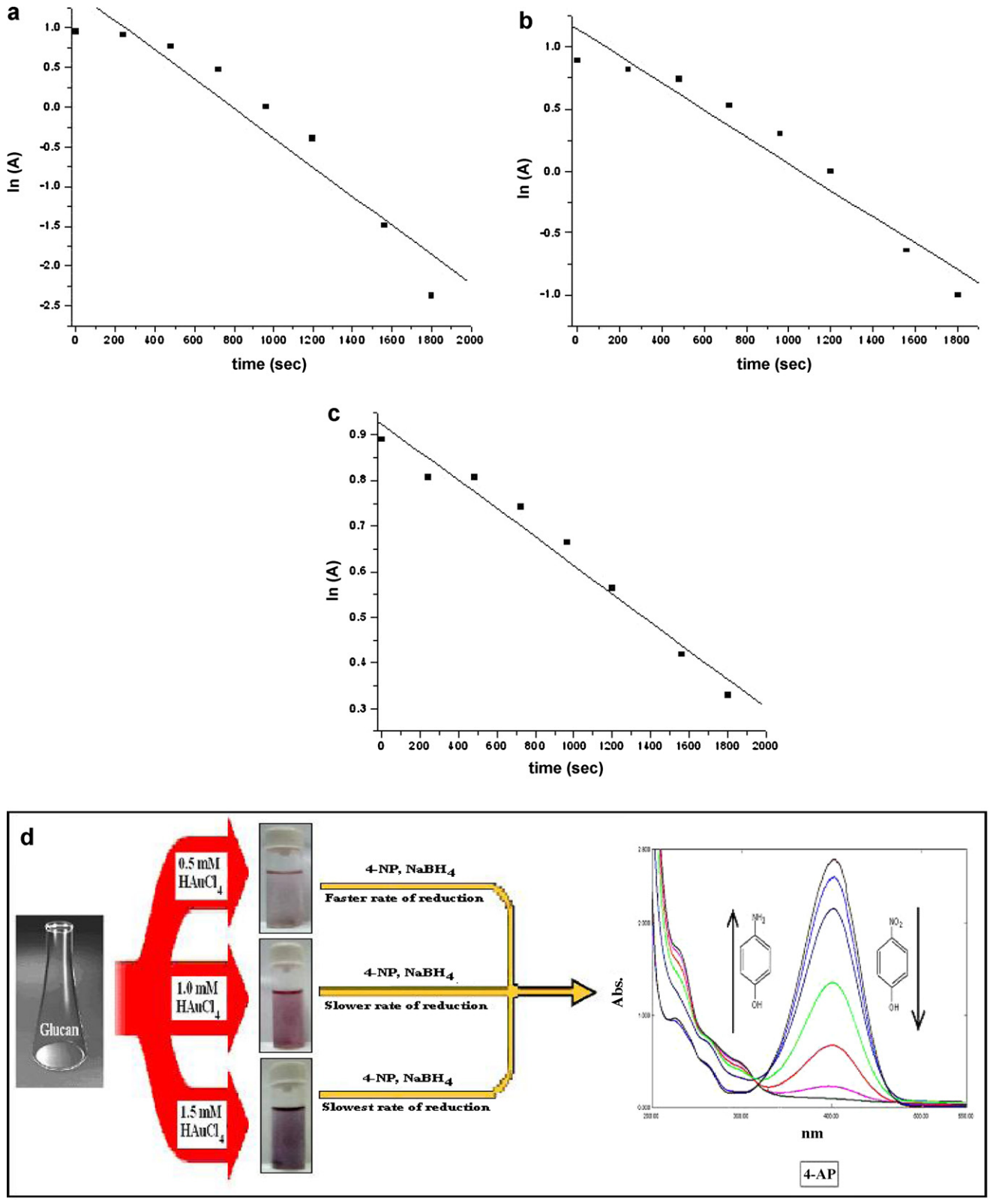

Fig. 7. Plot of ln(*A*) versus time for the catalytic reduction of 4-nitrophenol by Au NPs-glucan bioconjugates prepared with 0.05% (w/v) glucan and 0.5 mM $HAuCl_4$ (a) 1.0 mM $HAuCl_4$ (b) 1.5 mM $HAuCl_4$ (c). Schematic representation for the preparation of Au NPs-glucan bioconjugates and their function in the reduction of 4-nitrophenol (d).

particles in the reduction of 4-NP. This may be due to the fact that with the decrease in the size of Au NPs there is an increase in the number of low-coordinated Au atoms which promote the adsorption of the reactants (4-nitrophenolate ions and BH_4^-) on the catalyst surface and thereby facilitate the reduction. On the contrary, the larger particles are composed of relatively high-coordinated Au atoms related to lower surface roughness. The lower surface roughness is unfavorable for the adsorption of reactants and therefore does not facilitate the reduction (Wei et al., 2010). Thus, the particle size is the predominating factor over

Table 1a
Variation in the rate constant with variable size of Au NPs prepared with different $HAuCl_4$ concentrations and with a fixed glucan concentration.

Initial concentration of $HAuCl_4$ (mM)	Concentration of glucans (%, w/v)	Average size of the Au NPs (nm)	Rate constant, k (s^{-1})
0.5	0.05	5.33 ± 1.18	1.9×10^{-3}
1.0	0.05	8.01 ± 2.67	1.3×10^{-3}
1.5	0.05	14.93 ± 2.88	3.3×10^{-4}

Table 1b
Recent studies on the reduction rate of 4-NP over Au/polymer catalysts.

Entry	Polymer supports	Size of Au NP[a] (nm)	T[b] (K)	$NaBH_4$/4-NP/Au (mol/mol/mol)	k per Au content[c] (s^{-1} μmol Au^{-1})	Reference
1	PNIPAM-b-P4VP[d]	3.3	298	167/5/1	2.5×10^{-2}	Wang et al. (2007)
2	PMMA[e]	6.9	295	22,500/15/1	$7.2–7.9 \times 10^{-3}$	Kuroda, Ishida, and Haruta, (2009)
3	PDMAEMA-PS[f]	4.2	298	28/0.14/1	2.3×10^{-3}	Zhang et al. (2007)
4	Poly(DVB-*co*-AA)[g]	10	298	9800/267/1	4.1×10^{-2}	Liu, Wang, and Huang (2006)
5	Chitosan	3.1	303	20/6/1	5.0×10^{-3}	Chang and Chen (2009)
6	α-CD[h]	11	298	250/6/1	7.8×10^{-2}	Huang et al. (2009)
7	CSNFs[i]	5	298	15,000/150/1	5.9×10^{-1}	Koga et al. (2010)
8	α, β-D-glucan	8	298	207,360/3290/1	5.6×10^{-2}	Present work

[a] Observed by TEM.
[b] Reaction temperature.
[c] Pseudo-first-order reaction rate constant per Au content.
[d] Poly(*N*-isopropylacrylamide)-*b*-poly(4-vinylpyridine).
[e] Poly(methyl methacrylate).
[f] Poly(2-(dimethylamino)ethyl methacrylate) grafted on to solid polystyrene core.
[g] Poly(divinylbenzene-*co*-acrylic acid).
[h] α-Cyclodextrin.
[i] Cellulose single nanofibres.

loading effect in determining the catalytic activity of Au NPs prepared with glucan, isolated from an edible mushroom *P. florida*, cultivar Assam Florida. The overall observation is represented in a schematic representation (Fig. 7d). The Au NPs-glucan bioconjugates catalyst prepared with 1.0 mM $HAuCl_4$ was reused in successive cycles after recovery at the end of the reaction. The rate of reduction in the 1st and 2nd cycle was found to be 4.3×10^{-4} and 3.0×10^{-4} s^{-1}, respectively and in the 3rd cycle the reaction progressed with a very poor rate. Thus, the catalytic activity of the Au NPs-glucan bioconjugates gradually fall off during recycles and the reduction of 4-NP by $NaBH_4$ with this Au nanocatalyst could be done only up to the 2nd cycle compared to the system in which catalyst was absent. The decrease in catalytic activity during the successive cycles may be attributed to the deactivation of the active sites of catalyst by adsorbents (Wei et al., 2010).

4. Conclusions

For a healthy future of nanotechnology, green synthetic strategy should be adopted for nanoparticles synthesis using environmentally benign and renewable molecules to get rid of the hazards arising out of the use of chemical reducing agents and organic solvents. In this work, we have reported the green synthesis of Au NPs using a glucan, isolated from an edible mushroom *P. florida*, cultivar Assam Florida, which act as both reducing and stabilizing agent. The particles remain stable in aqueous solution even after two months of the reaction. The synthesized Au NPs-glucan bioconjugates exhibited excellent catalytic property in the reduction of toxic pollutant 4-nitrophenol to 4-aminophenol. Use of this Au NPs-glucan bioconjugates in the chemoselective reduction of some other nitrocompounds like isopthalic acids, and isomers of nitrobenzoic acids might be possible in future. The glucan used here has been isolated from a commercially available edible mushroom *P. florida*, cultivar Assam Florida. Hence, there might have a possibility for the large scale production of nanoparticles by using this glucan and application of the catalytic properties of Au NPs-glucan bioconjugates in industries.

Acknowledgements

The support rendered by the Department of Physics and Technophysics, Vidyasagar University for the XRD analysis is acknowledged. I.K.S. (one of the authors) thanks the CSIR, New Delhi, India for offering junior research fellowship (CSIR-09/599(042)/2011-EMR-I).

References

Anastas, P. T., & Warner, J. C. (1998). *Green chemistry: Theory and practice*. New York: Oxford University Press, Inc.
Babapour, A., Akhavan, O., Azimirad, R., & Moshfeg, A. Z. (2006). Physical characteristics of heat-treated nano-silvers dispersed in sol–gel silica matrix. *Nanotechnology*, *17*, 763–771.
Bo, L. L., Zhang, Y. B., Quan, X., & Zhao, B. (2008). Microwave assisted catalytic conversion of p-nitrophenol in aqueous solution using carbon-supported copper catalyst. *Journal of Hazardous Materials*, *153*, 1201–1206.
Bozanic, D. K., Djokovic, V., Blanusa, J., Nair, P. S., Georges, M. K., et al. (2007). Preparation and properties of nano-sized Ag and Ag_2S particles in biopolymer matrix. *The European Physical Journal E*, *22*, 51–59.
Cao, Y. W., Jin, R., & Mirkin, C. A. (2001). DNA-modified core–shell Ag/Au nanoparticles. *Journal of American Chemical Society*, *123*, 7961–7962.
Chang, Y.-C., & Chen, D.-H. (2009). Catalytic reduction of 4-nitrophenol by magnetically recoverable Au nanocatalyst. *Journal of Hazardous Materials*, *165*, 664–669.
Corma, A., & Serna, P. (2006). Chemoselective hydrogenation of nitro compounds with supported gold catalysts. *Science*, *313*, 332–334.
Dotzauer, D. M., Dai, J., Sun, L., & Bruening, L. M. (2006). Catalytic membranes prepared by using layer-by-layer adsorption of polyelectrolyte/metal nanoparticle films in porous supports. *Nano Letters*, *6*, 2268–2272.
Esumi, K., Takei, N., & Oshimura, T. Y. (2003). Antioxidant-potentiality of gold–chitosan nanocomposites. *Colloids and Surface B: Biointerfaces*, *32*, 117–123.
Ghosh, S. K., Mandal, M., Kundu, S., Nath, S., & Pal, T. (2004). Bimetallic Pt–Ni nanoparticles can catalyze reduction of aromatic nitrocompounds by sodium borohydride in aqueous solution. *Applied Catalysis A*, *268*, 61–66.
Hayward, R. C., Saville, D. A., & Aksay, I. A. (2000). Electrophoretic assembly of colloidal crystals with optically tunable micropatterns. *Nature*, *404*, 56–59.
Haruta, M., Kobayashi, T., Sano, H., & Yamada, N. (1987). Novel gold catalysts for the oxidation of the carbon monoxides at a temperature far below 0 °C. *Chemistry Letters*, *16*, 405–408.
Huang, T., Meng, F., & Qi, L. (2009). Facile synthesis and one-dimensional assembly of cyclodextrin-capped gold nanoparticles and their applications in catalysis and surface-enhanced Raman scattering. *Journal of Physical Chemistry C*, *113*, 13636–13642.

Koga, H., Tokunaga, E., Hidaka, M., Umemura, Y., saito, T., Isogai, A., et al. (2010). Topochemical synthesis and catalysis of metal nanoparticles exposed on crystalline cellulose nanofibres. *Chemical Communications*, *46*, 8567–8569.

Kuroda, K., Ishida, T., & Haruta, M. (2009). Reduction of 4-nitrophenol to 4-aminophenol over Au nanoparticles deposited on PMMA. *Journal of Molecular Catalysis A: Chemical*, *298*, 7–11.

Li, S., Shen, Y., Xie, A., Yu, X., Zhang, X., Yang, L., et al. (2007). Rapid, room-temperature synthesis of amorphous selenium/protein composites using *Capsicum annuum* L. extract. *Nanotechnology*, *18*, 405101, 9 pp.

Liu, W., Wang, X., & Huang, W. (2006). Catalytic properties of carboxylic acid functionlized-polymer microsphere-stabilized gold metallic colloids. *Journal of Colloid and Interface Science*, *304*, 160–165.

MaConnell, W. J., & Flinn, R. H. (1946). Summary of twenty-two trinitrotoluene fatalities in World II. *Journal of Industrial Hygiene*, *28*, 76–86.

Maity, K., Kar (Mandal), E., Maity, S., Gantait, S. K., Das, D., Maiti, S., et al. (2010). Structural characterization and study of immunoenhancing and antioxidant property of a novel polysaccharide isolated from the aqueous extract of a somatic hybrid mushroom of *Pleurotus florida* and *Calocybe indica* variety APK2. *International Journal of Biological Macromolecules*, *48*, 304–310.

Marais, E., & Nyokong, T. (2008). Adsorption of 4-nitrophenol onto Amberlite IRA-900 modified with metallophthalocyanines. *Journal of Hazardous Materials*, *152*, 293–301.

Mucic, R. C., Storhoff, J. J., Mirkin, C. A., & Letsinger, R. L. (1998). DNA-directed synthesis of binary nanoparticle network materials. *Journal of the American Chemical Society*, *120*, 12674–112675.

Mukherjee, P., Ahmad, A., Mandal, D., Senapati, S., Sankar, S. R., Khan, M. I., et al. (2001). Bioreduction of $AuCl_4^-$ ions by the fungus, *Verticillium* sp. and surface trapping of the gold nanoparticles formed. *Angewandte Chemie International Edition*, *40*, 3585–3588.

Nay, M. W., Randall, C. W., & King, P. H. (1974). Biological treatability of trinitrotoluene manufacturing waste water. *Journal of Water Pollution Control Federation*, *46*, 485–497.

Narayanan, K. B., & Sakthivel, N. (2011). Synthesis and characterization of nano-gold composite using *Cylindrocladium floridanum* and its heterogeneous catalysis in the degradation of 4-nitrophenol. *Journal of Hazardous Materials*, *189*, 519–525.

Oturan, M. A., Peiroten, J., Chartrin, P., & Acher, A. J. (2000). Complete destruction of p-nitrophenol in aqueous medium by electron-Fenton method. *Environmental Science and Technology*, *34*, 3474–3479.

Pastoriza-Santos, I., & Liz-Marzan, L. M. (1999). Formation and stabilization of silver nanoparticles through reduction by N,N-dimethylformamide. *Langmuir*, *15*, 948–951.

Philip, D. (2009). Biosynthesis of Au, Ag and Au–Ag nanoparticles using edible mushroom extract. *Spectrochimica Acta Part A: Molecular and Bimolecular Spectroscopy*, *73*, 374–381.

Philip, D. (2010). Green synthesis of gold and silver nanoparticles using *Hibiscus rosa sinensis*. *Physica E*, *42*, 1417–1424.

Pradhan, N., Pal, A., & Pal, T. (2001). Catalytic reduction of aromatic nitro compounds by coinage metal nanoparticles. *Langmuir*, *17*, 1800–1802.

Pradhan, N., Pal, A., & Pal, T. (2002). Silver nanoparticles catalyzed reduction of aromatic nitro compounds. *Colloids and Surface A: Physiochemical and Engineering Aspects*, *196*, 247–257.

Raveendran, P., Fu, J., & Wallen, S. L. (2003). Completely green synthesis and stabilization of metal nanoparticles. *Journal of the American Chemical Society*, *125*, 3940–13941.

Rivas, L., Sanchez-Cortes, S., Garcia-Ramos, J. V., & Morcillo, G. (2001). Growth of silver colloidal particles obtained by citrate reduction to increase the Raman enhancement factor. *Langmuir*, *17*, 574–577.

Roy, S. K., Das, D., Mondal, S., Maiti, D., Bhunia, B., Maiti, T. K., et al. (2009). Structural studies of an immunoenhancing water-soluble glucan isolated from hot water extract of an edible mushroom, *Pleurotus florida*, cultivar Assam Florida. *Carbohydrate Research*, *344*, 2596–2601.

Schmid, G. (2001). In K. J. Klabunde (Ed.), *Nanoscale materials in chemistry*. New York: Wiley.

Shi, Y., & Sun, X. (1988). *Spectrum and chemical identification of organic compounds*. Nanjing: Jiangsu Science Technology Press.

Sun, C., Qu, R., Chen, H., Ji, C., Wang, C., Sun, Y., et al. (2008). Degradation behavior of chitosan chains in the 'green' synthesis of gold nanoparticles. *Carbohydrate Research*, *343*, 2595–2599.

Tong, H. B., Xia, F. G., Feng, K., Sung, G. G., Gao, X. X., Sun, L. W., et al. (2009). Structural elucidation and immunological activity of a polysaccharide from the fruiting body of *Armillaria mellea*. *Bioresource Technology*, *100*, 1860–1863.

Tsutsui, Y., Hayakawa, T., Kawamura, G., & Nogami, M. (2011). Tuned longitudinal surface plasmon resonance and third-order nonlinear optical properties of gold nanorods. *Nanotechnology*, *22*, 275203.

Vigneshwaran, N., Kathe, A. A., Varadarajan, P. V., Nachane, R. P., & Balasubramanya, R. H. (2007). Silver-protein (core–shell) nanoparticle production using spent mushroom substrate. *Langmuir*, *23*, 7113–7117.

Wang, Y., Wei, G., Zhang, W., Jiang, X., Zheng, P., Shi, L., et al. (2007). Responsive catalysis of thermoresponsive micelle-supported gold nanoparticles. *Journal of Molecular Catalysis A: Chemical*, *266*, 233–238.

Wei, D., Ye, Y., Jia, X., Yuan, C., & Qian, W. (2010). Chitosan as an active support for assembly of metal nanoparticles and application of the resultant bioconjugates in catalysis. *Carbohydrate Research*, *345*, 74–81.

Zeng, F., Hou, C., Wu, S. Z., Liu, X. X., Tong, Z., & Yu, S. N. (2007). Silver nanoparticles directly formed on natural macroporous matrix and their anti-microbial activities. *Nanotechnology*, *18*, 8, 055605.

Zhang, M., Liu, L., Wu, C., Fu, G., Zhao, H., & He, B. (2007). Synthesis, characterization and application of well-defined environmentally responsive polymer brushes on the surface of colloid particles. *Polymer*, *48*, 1989.